Low frequency lumped element-based negative index metamaterial

Aycan Erentok and Richard W. Ziolkowski[a)]
Department of Electrical and Computer Engineering, University of Arizona, 1230 E. Speedway Blvd., Tucson, Arizona 85721-0104, USA

J. A. Nielsen, R. B. Greegor, C. G. Parazzoli, and M. H. Tanielian
Boeing Phantom Works, P.O. Box 3999, MC 3W-81, Seattle, Washington 98124-2499, USA

Steven A. Cummer, Bogdan-Ioan Popa, and Thomas Hand
Electrical and Computer Engineering Department, P.O. Box 90291, Duke University, Durham, North Carolina 27708, USA

D. C. Vier and S. Schultz
Department of Physics, University of California, San Diego, 9500 Gilman Drive, La Jolla, California 92093, USA

(Received 30 May 2007; accepted 9 October 2007; published online 2 November 2007)

A lumped element-based negative index metamaterial (NIM) was designed, fabricated, and tested for operation at 400 MHz in the ultrahigh frequency (UHF) band. At 400 MHz the measured real part of the index of refraction of this NIM was $n_{\text{real}}=-3.11$ with a loss that was less than 1 dB/cm using unit cells whose overall size d was $\lambda/d\sim 75$. The NIM bandwidth was $>10\%$ in the neighborhood of 400 MHz. © *2007 American Institute of Physics*. [DOI: 10.1063/1.2803771]

Metamaterials (MTMs) are artificial media whose constitutive parameters, in principle, can be engineered to achieve any specified value—either positive or negative. It has been discussed how electromagnetic waves can have counterintuitive properties in their interactions with metamaterials, e.g.,[1,2] particularly when the permittivities and permeabilities are negative. Volumetric MTMs have been realized mainly as composite artificial media formed by periodic arrays of dielectric or metallic inclusions located within or on a host substrate.[2] On the other hand, planar MTMs have been realized with lumped element-based transmission line structures.[3,4]

The increased interest in artificial materials has emerged mainly due to the unusual properties of the double negative (DNG) MTMs which have both $\varepsilon_{\text{real}}<0$ and $\mu_{\text{real}}<0$ and, consequently, a negative index of refraction $n_{\text{real}}<0$. When such negative index metamaterials (NIMs) are combined with double positive materials for which both $\varepsilon_{\text{real}}>0$ and $\mu_{\text{real}}>0$ and, consequently, $n_{\text{real}}>0$ (assuming low loss), they lead to a variety of interesting physical phenomena.[1–4] Nonetheless, many advantages of single negative (SNG) MTMs have also been reported. In particular, one application that utilizes either SNG or DNG MTMs is the proposed MTM-based paradigm to achieve efficient electrically small antennas (ESAs).[5–7] Many of the cases considered for efficient ESAs have been in the UHF band (300 MHz–3 GHz). Predictions of the radius of the sphere encompassing the entire radiating system have been on the order of 20 mm for 300 MHz, i.e., $r\sim\lambda/50$, with shell thicknesses on the order of 10 mm, i.e., $t\sim\lambda/100$, when an electric dipole antenna is surrounded with an epsilon-negative (ENG) material with $\varepsilon_{\text{real}}=-3.0\varepsilon_0$ or a DNG material with $n_{\text{real}}=-3.0$. For such ESAs, a NIM is required whose unit cell size d is on the order of or even smaller than 10 mm. Thus, the development of a NIM at UHF with low losses may have many practical applications. In this letter, we report the results obtained for a NIM which has $n_{\text{real}}\approx-3.0$ at 400 MHz with losses less than 1.0 dB/cm based on a maximum unit cell size $d\sim 10$ mm, i.e., $d\sim\lambda/75$.

It is well known[1–4] that one can use metallic patterns, such as split ring resonators and capacitively loaded loops, to achieve an effective negative permeability at microwave and UHF frequencies. On the other hand, it is challenging to achieve media with electrically small unit cell sizes that exhibit an effective ENG response at low frequencies and an effective mu-negative (MNG) response at high frequencies.

The NIM design we developed is shown in Fig. 1(a). The ENG part of the design [Fig. 1(b)] was based on the lumped element meanderline design presented in Ref. 8; the MNG part [Fig. 1(c)] was a lumped element version of the capacitively loaded loop volumetric artificial magnetic conductor MTM presented in Ref. 9. The NIM design consisted of a unit cell with the following layers: (a) a two-dimensional meander integrated with a lumped element inductor to realize the ENG portion of the unit cell, (b) a two-dimensional rectangular loop integrated with a lumped element capacitor to realize the MNG portion of the unit cell, and (c) Rohacell™ layers. The Rohacell™ layers provided physical separation of the ENG and MNG portions, as well as physical support to the entire NIM unit cell. Their thicknesses were utilized to adjust the effective permittivity and permeability values of the unit cell to the desired values, in part by tailoring the significant electromagnetic interactions between the ENG and MNG portions of the unit cell. The lumped element inductor (capacitor) provided the extra inductance (capacitance) to the meander (loop) structure to further shift its resonance behavior to lower frequencies, while maintaining a small unit cell size. The final design was reached after several series of simulations produced with Ansoft's high frequency structure simulator (HFSS) combined with Ansoft Designer and with CST's microwave studio (MWS), as well as with measurements of the corresponding preliminary design slabs. The design specifications of the measured NIM design are given in Figs. 1(b) and 1(c).

[a)]Electronic mail: ziolkowski@ece.arizona.edu

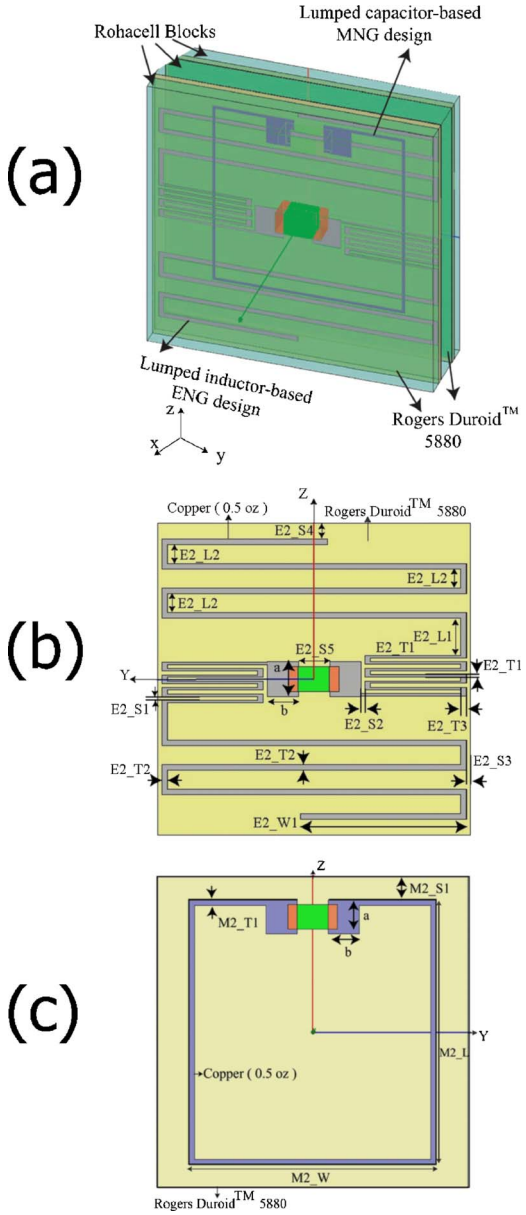

FIG. 1. (Color online) Detailed design specifications of the NIM design: (a) NIM unit cell, (b) ENG unit cell realization based on a 2D meanderline integrated with a lumped element inductor, and (c) MNG unit cell realization based on a 2D rectangular loop integrated with a lumped element capacitor.

The indicated ENG unit subcell specifications for the NIM design were E2_S1=E2_S2=E2_S3=0.127 mm, E2_S4=0.385 mm, E2_S5=1.0 mm, E2_T1=0.0762 mm, E2_T2=E2_T3=0.1778 mm, E2_L1=1.1938 mm, E2_L2 =0.6096 mm, and E2_W1=5.3 mm; the corresponding MNG unit subcell specifications were M2_W=6.476 mm, M2_L=6.572 mm, M2_T1=1.746 mm, M2_S1=1.577 mm; and the Rohacell™ unit cell thickness value was 1.0 mm. The total thickness along the x axis was 2.542 mm. Therefore, the overall NIM unit cell size was $2.542\times10\times10$ mm^3. Note that the lumped elements were embedded into the Rohacell™ layers by introducing rectangular cutouts for these elements in those layers. This approach allowed us to decrease the overall thickness of the NIM unit cell.

A slab of this NIM design was fabricated and tested. The ENG portion of the NIM unit cells contained two meanderlines, one connected to each end of a centered lumped element inductor. The inductors for the final designs were obtained from Murata and had the specified value of 470 nH, ±5%. The MNG portion contained a rectangular loop loaded with a lumped element capacitor. The capacitors for the final designs were also obtained from Murata and had the specified values 5.6±0.25 pF. All of the boards used to realize the unit cell structures were fabricated on Rogers 5880 Duroid™ material. The boards were 10 mils (0.254 mm) thick with 0.5 oz. copper (~17 μm thick metal layers). The solder pads had the dimensions $a\times b=1.1\times1.0$ mm^2. The front sides of the boards were etched to achieve the desired pattern of the copper; the backsides of the boards were blanket etched to remove all of the copper. The finished boards were laser cut into three by three arrays of unit cells with a CO_2 laser. The fabricated ENG unit cell portion, Rohacell™ spacer, and MNG unit cell portion are shown in Figs. 2(a)–2(c), respectively. Once the boards were laser cut, the passives were soldered into place. Solder stencils were used to control the pattern and thickness of the solder paste, followed by vapor phase solder reflow. This method allows for less solder and the results are more repeatable than hand soldering. We also considered the use of a solder mask to limit the flow of the solder paste during the reflow process, but rejected this idea since the solder mask remains on the board after the reflow process. It was our belief that having the solder mask between the arms of the meander would have increased the losses in the NIM structure. The entire slab was covered with Top Flite MonoKote®, a heat shrinkable plastic. This material does not affect the losses and has been used in many past designs for mechanical stability.[10] The fabricated slab is shown in Fig. 2(d). An ENG-only unit cell metamaterial slab based on this NIM cell without the MNG elements was also fabricated and tested. It confirmed the ENG behavior of this portion of the NIM unit cell.

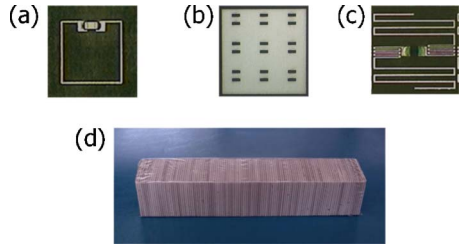

FIG. 2. (Color online) Photographs of the fabricated NIM design: (a) the MNG portion of the unit cell, (b) the 3×3 unit cell Rohacell spacer with cutouts for embedding the lumped elements, (c) the ENG portion of the unit cell, and (d) the final assembled $3\times3\times15$ cm^3 NIM slab.

This UHF MTM slab was designed to be excited by an electromagnetic wave propagating along the y direction of Fig. 1 with its electric and magnetic fields, respectively, polarized along the z and x directions. Since a free space measurement of the transmission properties of a sample at 400 MHz requires a large sample and a correspondingly large free space test range, we opted to make the measurement in an UHF waveguide. A two conductor transverse electric and magnetic (TEM) microstrip waveguide with 3 cm plate separation, 15 cm top plate width was chosen so that the metamaterial sample described above ($3\times3\times15$ cm^3) filled the entire cross-sectional area of the waveguide. The separation and width of the plates were tapered to maintain a 50 Ω characteristic impedance along the entire length of the waveguide. This open, two conductor wave-

guide has no lower cutoff frequency and is capable of measurements from DC to 5 GHz, where the waveguide finally becomes multimode. Calibration testing with slabs of known permittivity and permeability, such as Rexolite™, yielded good results from 150 MHz to 2 GHz. Closed rectangular waveguides have been used for metamaterial characterization at higher frequencies,[11,12] but such a waveguide at 400 MHz would require prohibitively large material samples. Since this microstrip waveguide supports a TEM plane wave that is normally incident on the slab under test, the measured complex S parameters were converted to the effective complex permittivity and permeability of the slab using the approach given in Ref. 13. This approach required reflection and transmission coefficients defined at the boundaries of the slab, and the slab was deembedded from the waveguide through S-parameter measurements of a metal plate placed at the same location as the slab. Because the wavelength at 400 MHz is long, the precision required in the placement of this slab was not stringent. Some care was taken in the extraction of the effective permittivity and permeability of the metamaterial slab from the measured S parameters because of ambiguities introduced by the multivalued arccosine function.[13] However, provided that the slabs are electrically thin and passive [i.e., so that the sign of $\mathrm{Im}(n)$ is known], as they were in the cases considered in this investigation, these ambiguities were easily resolved. The final result was the measurement of a unique effective permittivity and permeability of the slab under test.

The loss was obtained in two ways. It was obtained from the extracted index of refraction as

$$\text{loss (dB/cm)} = -10\log 10\left[\exp(-2.0\times 2\pi f\,\mathrm{Im}(n)d_{\mathrm{slab}}/c)\right]/d_{\mathrm{slab}}, \quad (1)$$

where d_{slab} is the thickness of the slab. The loss value was also obtained directly from the measured and predicted S parameters as

$$\text{loss (dB/cm)} = -10\log 10\left(\frac{|S_{21}|^2}{1-|S_{11}|^2}\right)\Big/ d_{\mathrm{slab}}. \quad (2)$$

The agreement between the two approaches was very good in all of the simulated and measured cases.

The measured index of refraction results for the NIM design slab are shown in Fig. 3(a) for the entire frequency band and in Fig. 3(b) for frequencies in the immediate neighborhood of the target frequency. The fabricated NIM slab was measured to have $n_{\mathrm{real}}=-3.11$ at 400 MHz with a 0.91 dB/cm loss value. The effective unit cell size was $d=\lambda/75$. The wave impedance of the slabs was calculated in all the slabs manufactured. The measured impedance of the NIM design slab shown in Fig. 3 normalized to the free-space impedance was 0.756. This means the power accepted by the slab was 98.07% of the incident power. Future designs could have the NIM slab matched to free space to maximize the power accepted by the slab.

It was found that the actual lumped element capacitance and inductance values had a significant impact on the final NIM performance. Higher quality components with lower parameter tolerances would enhance the design cycle, particularly to achieve acceptable comparisons between the simulation and experimental results. Additional simulations showed that the majority of the losses in these designs originated in the lumped elements and in the very thin copper traces. We believe that with improved components even lower loss UHF NIM materials can be fielded for a variety of practical applications.

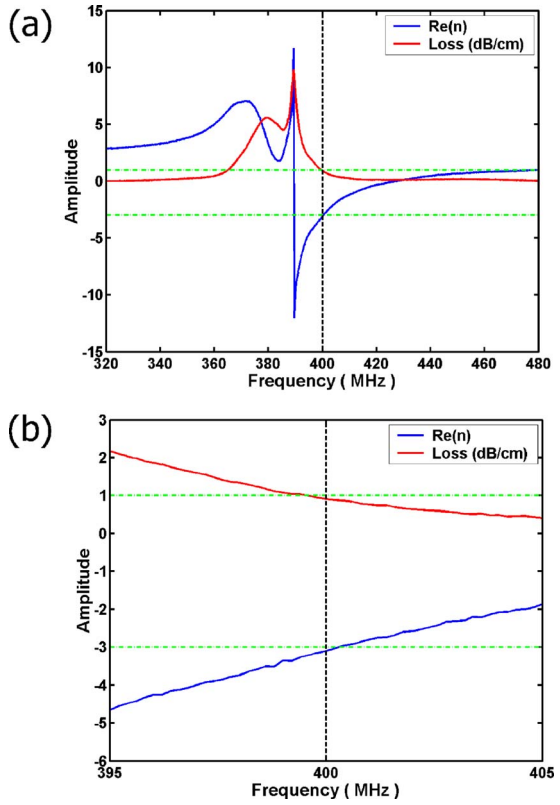

FIG. 3. (Color online) Measured index of refraction values obtained for the NIM design unit cell structure: (a) entire measured frequency band and (b) zoom, showing that at 400 MHz the real part of the refractive index is ~ -3 with a loss <1 dB/cm.

This work was supported in part by DARPA under Contract No. HR0011-05-C-0068.

[1] N. Engheta and R. W. Ziolkowski, IEEE Trans. Microwave Theory Tech. **53**, 1535 (2005).
[2] *Metamaterials: Physics and Engineering Explorations*, edited by N. Engheta and R. W. Ziolkowski (IEEE, New York/Wiley, New York, 2006).
[3] C. Caloz and T. Itoh, *Electromagnetic Metamaterials: Transmission Line Theory and Microwave Applications* (IEEE, New York/Wiley, New York, 2005).
[4] *Negative Refraction Metamaterials: Fundamental Properties and Applications*, edited by G. V. Eleftheriades and K. G. Balmain (IEEE, New York/Wiley, Hoboken, NJ, 2005).
[5] R. W. Ziolkowski and A. Erentok, IEEE Trans. Antennas Propag. **54**, 2113 (2006).
[6] R. W. Ziolkowski and A. Erentok, IET Proc. Microwaves, Antennas Propag. **1**, 116 (2007).
[7] A. Erentok and R. W. Ziolkowski, IEEE Trans. Antennas Propag. **55**, 731 (2007).
[8] P. Imhof, "Metamaterial-based Epsilon Negative (ENG) Media: Analysis and Designs," M.S. thesis, EPFL, 2006.
[9] A. Erentok, P. Luljak, and R. W. Ziolkowski, IEEE Trans. Antennas Propag. **53**, 160 (2005).
[10] R. B. Greegor, C. G. Parazzoli, J. A. Nielsen, M. A. Thompson, M. H. Tanielian, D. C. Vier, S. Schultz, D. R. Smith, and D. Schurig, IET Proc. Microwaves, Antennas Propag. **1**, 108 (2007).
[11] S. A. Cummer and B.-I. Popa, Appl. Phys. Lett. **85**, 4564 (2004).
[12] H. Chen, J. Zhang, Y. Bai, Y. Luo, L. Ran, Q. Jiang, and J. A. Kong, Opt. Express **14**, 12944 (2006).
[13] D. R. Smith, S. Schultz, P. Markos, and C. M. Soukoulis, Phys. Rev. B **65**, 195104 (2002).